

## Direct Experimental Observation of the Crossover from Capillary to Elastic Surface Waves on Soft Gels

Francisco Monroy\*<sup>†</sup> and Dominique Langevin<sup>†</sup>

Centre de Recherche Paul Pascal, CNRS, Avenue Dr. Schweitzer, Château Brivazac, F-33600 Pessac, France

(Received 28 May 1998)

By using electrically excited surface waves we have studied the propagation of hydrodynamic modes on the surface of agarose gels in the frequency range  $10^1$ – $10^3$  Hz. Bulk rheological behavior has been also determined in the frequency range  $10^{-2}$ – $10^2$  Hz by conventional rheometry. The propagation of two surface modes, capillary and elastic, is observed at low frequencies. Above a well defined crossover frequency, regular capillary behavior is observed. The experimental data are in excellent agreement with the theoretical predictions and the measured bulk viscoelastic behavior. [S0031-9007(98)07302-5]

PACS numbers: 62.30.+d, 47.35.+i, 68.10.Et, 82.70.Gg

The hydrodynamic behavior of bulk viscoelastic systems has been the subject of extensive studies in the last decades [1]. The surface hydrodynamics of these materials is experimentally accessible thanks to quasielastic surface light scattering (QESLS) and excited surface waves (ESW) techniques [2]. This special hydrodynamics is relevant to various applications, such as energy dissipation in lubricants by means of bulk-surface energy transfer, or the observation of anomalous turbulent flow through polymer gel-coated capillaries [3]. In order to describe theoretically this hydrodynamics, Harden, Pleiner, and Pincus (hereinafter, HPP theory) [4] proposed in 1991 the extension to viscoelastic fluids of the classical description of surface waves [5], which frequency and damping are governed by surface tension  $\gamma$  and fluid shear viscosity  $\eta$ . This extension is performed by substituting formally the shear viscosity by  $\eta^*(\omega) = \eta(\omega) + E(\omega)/i\omega$ , where  $\eta(\omega)$  and  $E(\omega)$  are the shear viscosity and shear modulus, respectively, and  $\omega = 2\pi\nu$ ,  $\nu$  being the frequency. The new feature emerging from this theory is the coexistence of several types of surface modes. The regimes where these modes are observed are represented in Fig. 1. Capillary waves, either Kelvin waves ( $\omega_q \sim q^{3/2}$ ), or overdamped nonpropagating ( $\omega_q \sim iq$ ) waves and Rayleigh or elastic waves ( $\omega_q \sim q$ ), can be observed, depending on bulk viscoelasticity and frequency. Pure capillary modes are found in the low shear modulus solutions. The damping of these modes increases if the frequency or the shear viscosity increases, until the modes are overdamped. At high shear modulus values and at low frequencies, Rayleigh modes are found. Obviously, the boundaries shown in Fig. 1 are not sharp, and the transitions between the different types of modes are smooth. Capillary and Rayleigh modes can eventually coexist, propagating together in space and time. This particular feature leads in principle to the presence of two peaks in the QESLS spectra, corresponding to each mode [4]. The HPP theory has been recently extended to account for the presence of surface adsorption by Wang *et al.* [6].

The search for Rayleigh surface modes has been the subject of a great quantity of work. Polymer gels are good candidates for the observation of mode coexistence. They are soft solids made of polymer chains entangled in a network structure with a zero frequency shear modulus increasing as the polymer concentration increases. The first indirect evidence of Rayleigh modes was early reported by Cummins *et al.* [7] who studied polyisobutylene solutions in decane (PIB/D) with QESLS, and reported an evolution of the potential law for peak frequency  $\omega_q \sim q^n$  when the polymer concentration increases:  $n \sim 1.5$  at low concentrations, typical of capillary modes, and  $n \sim 1.0$  at high concentrations, typical of elastic Rayleigh modes. However, Dorshow and Turkevich showed that a similar evolution is expected during the transition from propagating to overdamped capillary modes [8], and presented later new data on PIB solutions in hexane, where a noticeable increase in the peak frequency with polymer concentration is observed while the solution becomes viscoelastic [9], another indirect evidence of a crossover to an elastic regime. Afterwards, Cummins *et al.* reported new data on polyethyleneoxide (PEO) aqueous solutions showing the same behavior, together with a decrease of the spectral width, despite a rapid increase of the bulk viscosity

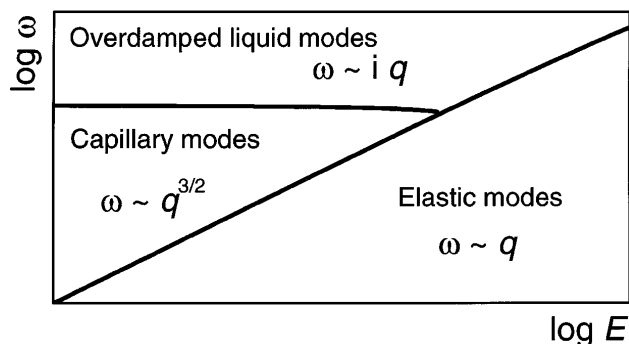


FIG. 1. Surface mode diagram for viscoelastic gels.

[10], an observation also consistent with a crossover from capillary to elastic regime. However, in all the above experiments, the spectral noise prevented the observation of the two peaks predicted in HPP theory. Moreover, PEO is surface active, and although the surface tension remains essentially independent of the polymer concentration in the studied range, surface elasticity and viscosity are expected to change significantly the propagation characteristics of the surface waves [6]. Huang and Wang have carried out QESLS experiments with polyvinylpyrrolidone aqueous solutions [11] and very recently on PIB solutions in decane, with polymer molecular weights larger than Cummins *et al.* [12]. Their data are fully consistent with HPP theory. However, the distinctive bimodal features manifested in the theoretical spectra are smeared out by the instrumental broadening and are not distinguishable in the experimental spectra. In fact, the observation of two peaks is difficult at the high frequencies of the QESLS technique, because the gels need to have at the same time a high elastic modulus and small viscosity. Kikuchi *et al.* [13] and Choi [14] combined QESLS and ESW to extend the frequency range of the experiments down to 100 Hz. In their ESW method, the surface is distorted by a pulsed mechanical excitation and the phase velocity  $c$  of the pulse is deduced from the phase shift of the surface displacement at a distance  $d$  from the source of excitation. This study clearly showed the complete crossover from the capillary regime  $c = \omega/q \sim q^{1/2}$  to the elastic regime where  $c$  is frequency independent. Unfortunately, the ESW method used only gives an average value of  $c$  and is unable to allow the observation of two modes.

At this point, the ESW method with electrocapillary excitation seemed to us a suitable technique, because of its noninvasive character and because the surface displacement profile  $\zeta(x)$  along wave propagation direction is directly obtained. Our experimental setup has been described elsewhere [15]. We have studied 0.2 wt % aqueous solutions of agarose (Fluka) prepared by dissolving the powder in de-ionized water from a Milli-Q system at high temperature ( $\sim 90^\circ\text{C}$ ). During the dissolution process, extremely gentle agitation was maintained in order to prevent any shear degradation. After complete dissolution, the hot solution was transferred to the Langmuir trough, leaving it to stabilize at room temperature ( $22.0 \pm 0.5^\circ\text{C}$ ). The samples showed no substantial volume change through the gelation process. The density is  $1.0 \text{ g cm}^{-3}$  for all the samples. No change in surface wave propagation characteristics was observed over 4 h intervals. ESW experiments were performed at different frequencies. The exciting voltage was kept constant in a linear deformation regime (the maximum surface deformation is less than  $1 \mu\text{m}$ ).

For the sake of brevity only three spatial profiles obtained at different excitation frequencies are shown in Fig. 2. The existence of two different modes is evident in Fig. 2(b). In order to check for possible reflections

at the borders of the trough, which could yield spurious bimodal behavior, we have used two different Langmuir troughs (15 and 70 cm long, respectively). We have obtained identical profiles in both cases (see also Fig. 3). Fourier transformation of the experimental profiles  $\zeta(x)$  was performed by the fast-Fourier-transform (FFT) algorithm, revealing clearly single or bimodal distributions depending on frequency. In fact, at  $\nu > 200 \text{ Hz}$ , we observed invariably a single component damped sinusoidal behavior, easily recognizable by the presence of a single peak in the spectrum  $P(q) = FT\{\zeta(x)\}$ . Close to  $\nu = 200 \text{ Hz}$ , a second peak emerges with a smaller wave vector than the capillary peak, moving away from this peak as the frequency decreases. It is obvious in Fig. 2 that mode mixing at the crossover is much easier to see in the  $\zeta(x)$  signal than on its Fourier transform. This peculiarity, together with the frequency range and the instrumental broadening inherent to the QESLS technique, explains why this technique is not as well suited as ESW

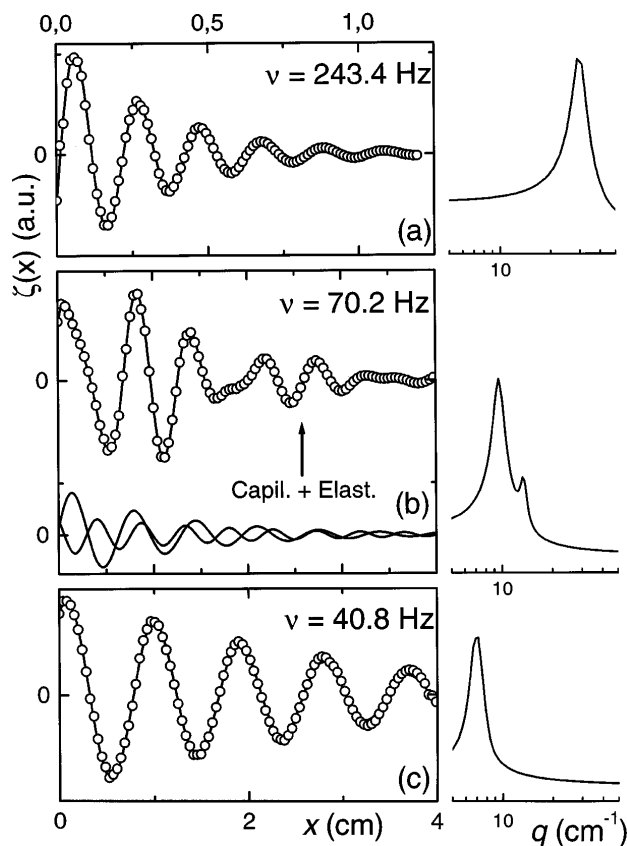


FIG. 2. Experimental surface profiles of an agarose solution 0.2 wt % at three different excitation frequencies, showing a pure capillary mode (a), mixed crossover behavior (b), and a pure elastic mode (c). The experimental points have been fitted to the expression given in Eq. (1) (continuous line). Only 100 of the 2000 experimental points are represented for clarity. The amplitude of the two different components is also represented in the bottom of (b). Fourier transformations of the experimental profiles are represented in the right.

to study the bimodal behavior. When the polymer concentration increases further, the relative amplitude of the elastic peak increases, but the capillary peak does not disappear completely in the frequency range studied; at the lowest frequency,  $\nu \sim 40$  Hz, the capillary contribution is still of order 20%. The relative amplitude of the modes is related to the energy distribution between modes and requires further analysis within HPP theory. This question is out of the scope of this Letter, and will be discussed in a subsequent publication. The amplitude of the normalized experimental profiles has been fitted to the following bimodal distribution by using a nonlinear minimum squares algorithm

$$\zeta(x) = \sum_{j=1,2} A_j \cos(q_j x + \phi_j) \exp(-\alpha_j x), \quad (1)$$

where  $j = 1$  corresponds to the capillary mode and 2 to the elastic one,  $q_j$  is the wave vector, and  $\alpha_j$  the spatial damping;  $\phi_j$  accommodates the nonzero phase at origin derived from the finite distance between the arbitrary departure point  $x = 0$  and the excitation source.

As expected, at high frequency we find single mode behavior ( $A_2 \sim 0$ ) and emerging bimodal behavior when reaching the low frequency domain  $\nu \leq 200$  Hz. For still smaller frequencies ( $\nu \leq 80$  Hz) a regime of dominating single mode behavior is observed, with amplitudes of  $A_1 \sim 0.2$  and  $A_2 \sim 0.8$ , respectively. The success of these fits is clearly evidenced in Fig. 2(b) where we have incorporated the two independent modes and their sum, which is able to describe successfully the experimental profile, its strange composite damping, and the exact position of the "phantom" or false zeros. Unambiguously, this is the first reported direct observation of mode coexistence predicted by HPP theory.

Figure 3 shows the values of the phase velocity  $c$ , obtained from these fits to the experimental profiles. First of all, these data demonstrate the high degree of reproducibility of the experiments and the negligible influence of wall effects in the smaller trough. As expected, the dispersion curve scales exactly as  $\sim \omega^{1/3}$ , and separates

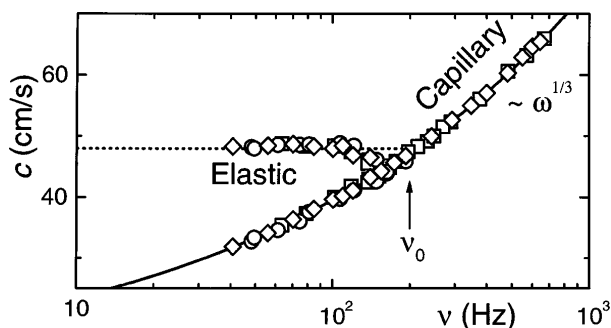


FIG. 3. Phase velocity for surface modes of 0.2 wt % agarose solutions. The three independent series correspond to different samples studied in the small (O) or large trough ( $\Delta$ ). The so-called capillary branch shows a well defined  $\omega^{1/3}$  behavior as given in Eq. (3) (continuous line).

into two branches corresponding to the two modes at a crossover frequency  $\nu_0 = 200$  Hz. In order to assign each branch to a given mode, it is necessary to compare its velocity with the theoretical predictions. For this purpose, bulk rheological measurements were performed with a cone-plate mechanical rheometer (Rheometrics). Figure 4 shows the frequency dependence of the complex viscoelastic modulus  $G(\omega) = i\omega\eta^*(\omega) = E(\omega) + i\omega\eta(\omega)$ .

The nonzero values of the shear modulus are the irrefutable signature of the gel state, and there is little dependence of  $E$  and  $\omega\eta$  on frequency. As seen from Fig. 4, the studied agarose gel shows low shear viscosity and high elastic modulus at moderate frequencies ( $\nu \leq 100$  Hz), being hence an ideal system for the search of the elastic modes. In the HPP formalism the complete dispersion equation is given by the following expression:

$$D(q, \omega) = \frac{\gamma}{\rho} q^3 + (i\omega + \Theta)^2 - \Theta^2 \sqrt{1 + 2i\omega/\Theta} = 0, \quad (2)$$

where  $\Theta = 2\eta^*(\omega)q^2/\rho$ .

In the limit of very small viscosities ( $y = \gamma\rho/4\eta^2q \gg 1$ ), and if elastic or capillary effects are negligible, the phase velocity of surface modes is, respectively, given by [16]

$$c_C \approx \left(\frac{\gamma}{\rho}\omega\right)^{1/3} \quad c_E \approx 2\left(\frac{E}{\rho}\right)^{1/2}. \quad (3)$$

Experimentally, pure capillary behavior ( $c \sim \omega^{1/3}$ ) was found in all cases above 200 Hz and in the low velocity branch (high  $q$ ) of the low frequency data. By using Eq. (3) for  $c_C$ , one obtains  $\gamma = 71.5 \pm 1.2$  dyn cm $^{-1}$ , close to pure water value as it would be expected since the agarose chains are not surface active [17]. We have independently measured the contact angles of sessile drops of water and of agarose gels on Teflon, and found that they were the same, thus confirming the absence of any agarose adsorption at the gel surface. On other hand, the high velocity branch in Fig. 3, essentially independent of

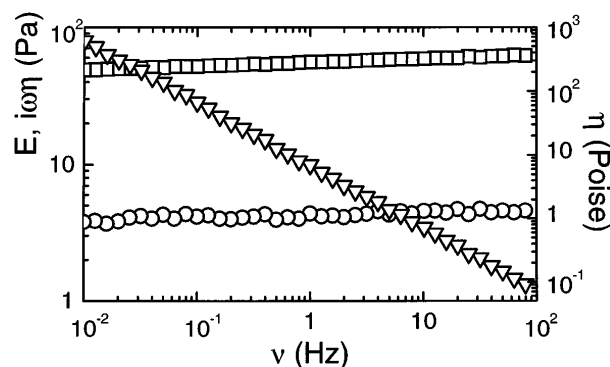


FIG. 4. Rheological data  $E(\omega)$  ( $\square$ ),  $i\omega\eta$  ( $\circ$ ), and shear viscosity  $\eta(\nu)$  of 0.2 wt % agarose gels at  $22.0 \pm 0.1$  °C.

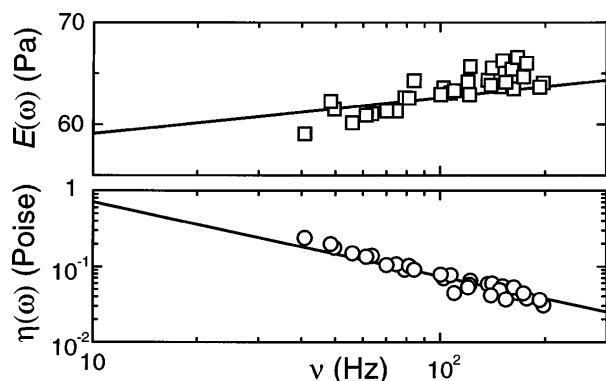


FIG. 5. Shear modulus ( $\square$ ) and shear viscosity ( $\circ$ ) of 0.2 wt% agarose solutions, obtained from propagation characteristics of surface elastic modes by using the complete HPP dispersion equation [Eq. (2)]. For comparison, data obtained from bulk mechanical measurements (continuous lines) have been incorporated.

$\omega$ , is obviously compatible with Rayleigh-like behavior as is given in Eq. (3), from which one obtains  $E \sim 58$  Pa at  $\nu = 100$  Hz, very close to the real value at the same frequency equal to 62.6 Pa. It is possible to give also a theoretical estimation of crossover frequency  $\nu_0$  at which  $c_C = c_E$ , by using

$$q_0 \approx 4 \frac{E}{\gamma} \quad \nu_0 \approx \frac{8}{2\pi} \frac{E^{3/2}}{\gamma \rho^{1/2}}. \quad (4)$$

With  $\gamma \approx 72$  dyn cm $^{-1}$  and  $E \approx 63$  Pa one obtains  $q_0 \approx 35$  cm $^{-1}$  and  $\nu_0 \approx 275$  Hz, which are in excellent agreement with the observed position of the crossover point, placed at 20 cm $^{-1}$  and 200 Hz, respectively. After checking for these simple approximations, we have performed a rigorous numerical comparison between data and theory. We have calculated both elasticities and viscosities by comparing the complete wave characteristics (frequency and damping) to the dispersion equation [Eq. (2)] and by assuming that the surface tension has the value of pure water which we have measured at room temperature:  $\gamma = 72.4$  dyn/cm. The results are shown in Fig. 5. One sees that there is a remarkable agreement between the ESW experiments, the rheological data, and the HPP theory.

In conclusion, the present experiment is the first direct observation of the coexistence of two surface modes

in the crossover region, the usual capillary mode, and the Rayleigh elastic mode. At higher frequencies, pure capillary regime is reached. The data are in excellent quantitative agreement with the theory of Harden, Pleiner, and Pincus when shear elasticities and viscosities determined independently at the same frequencies with conventional rheometers are used to analyze the surface wave characteristics.

F.M. was supported by European Community under a postdoctoral TMR Contract ERBFMBICT960872.

\*Author to whom correspondence should be addressed.

†Present address: Laboratoire de Physique des Solides, Bâtiment 510, Université Paris-Sud, 91405 Orsay, France.

- [1] M. Doi and S.F. Edwards, *The Theory of Polymer Dynamics* (Oxford University Press, New York, 1986).
- [2] *Light Scattering by Liquid Surfaces and Complementary Techniques*, edited by D. Langevin (Dekker, New York, 1992).
- [3] A. Silberberg, *PhysicoChem. Hydrodyn.* **9**, 419 (1987).
- [4] J.L. Harden, H. Pleiner, and P.A. Pincus, *J. Chem. Phys.* **94**, 5208 (1991).
- [5] V.G. Levich, *Physicochemical Hydrodynamics* (Prentice Hall, Englewood Cliffs, NJ, 1962).
- [6] C.H. Wang and Q.R. Huang, *J. Chem. Phys.* **107**, 5898 (1997).
- [7] B.H. Cao, M.W. Kim, H. Schaffer, and H.Z. Cummins, *J. Chem. Phys.* **95**, 9317 (1991).
- [8] R.B. Dorshow and L.A. Turkevich, *J. Chem. Phys.* **98**, 8349 (1993).
- [9] R.B. Dorshow and L.A. Turkevich, *Phys. Rev. Lett.* **70**, 2439 (1993).
- [10] B.H. Cao, M.W. Kim, and H.Z. Cummins, *J. Chem. Phys.* **102**, 9375 (1995).
- [11] Q.R. Huang and C.H. Wang, *J. Chem. Phys.* **105**, 6546 (1996).
- [12] Q.R. Huang, C.H. Wang, and N.J. Deng, *J. Chem. Phys.* **108**, 3827 (1998).
- [13] H. Kikuchi, K. Sakai, and K. Takagi, *Phys. Rev. B* **49**, 3061 (1994); *Jpn. J. Appl. Phys.*, **30**, L1668 (1991).
- [14] P.K. Choi, *Jpn. J. Appl. Phys.* **31**, 54 (1992).
- [15] C. Stenvot and D. Langevin, *Langmuir* **4**, 1179 (1988).
- [16] L.D. Landau and E.M. Lifshitz, *The Theory of Elasticity* (Pergamon Press, New York, 1959).
- [17] C.J. van Oss, *Interfacial Forces in Aqueous Media* (Dekker, New York, 1994).